Acknowledgements

The assistance of GLAD-IPNS beamline scientists Y. Badyal and C. Benmore is gratefully acknowledged. This work was supported by the NSF, and the US DOE-BES Division of Materials Sciences. J. D. M. is a Cottrell Scholar of the Research Corporation.

Competing interests statement

The authors declare competing financial interests: details accompany the paper on *Nature*'s website (http://www.nature.com/nature).

Correspondence and requests for materials should be addressed to J.D.M. (e-mail: jdmartin@ncsu.edu).

Self-organization of supramolecular helical dendrimers into complex electronic materials

V. Percec*, M. Glodde*, T. K. Bera*, Y. Miura*, I. Shiyanovskaya† K. D. Singer†, V. S. K. Balagurusamy*‡, P. A. Heiney‡, I. Schnell§, A. Rapp§, H.-W. Spiess§, S. D. Hudson‖ & H. Duan‖

** Roy & Diana Vagelos Laboratories, Department of Chemistry, University of Pennsylvania, Philadelphia, Pennsylvania 19104-6323, USA*
† Department of Physics, Case Western Reserve University, Cleveland, Ohio 44106-7079, USA
‡ Department of Physics and Astronomy, University of Pennsylvania, Philadelphia, Pennsylvania 19104-6323, USA
§ Max Planck Institute for Polymer Research, D-55021 Mainz, Germany
‖ National Institute of Standards and Technology, Gaithersburg, Maryland 20899-8544, USA

The discovery of electrically conducting organic crystals[1] and polymers[1–4] has widened the range of potential optoelectronic materials[5–9], provided these exhibit sufficiently high charge carrier mobilities[6–10] and are easy to make and process. Organic single crystals have high charge carrier mobilities but are usually impractical[11], whereas polymers have good processability but low mobilities[1,12]. Liquid crystals exhibit mobilities approaching those of single crystals and are suitable for applications[13–18], but demanding fabrication and processing methods limit their use. Here we show that the self-assembly of fluorinated tapered dendrons can drive the formation of supramolecular liquid crystals with promising optoelectronic properties from a wide range of organic materials. We find that attaching conducting organic donor or acceptor groups to the apex of the dendrons leads to supramolecular nanometre-scale columns that contain in their cores π-stacks of donors, acceptors or donor–acceptor complexes exhibiting high charge carrier mobilities. When we use functionalized dendrons and amorphous polymers carrying compatible side groups, these co-assemble so that the polymer is incorporated in the centre of the columns through donor–acceptor interactions and exhibits enhanced charge carrier mobilities. We anticipate that this simple and versatile strategy for producing conductive π-stacks of aromatic groups, surrounded by helical dendrons, will lead to a new class of supramolecular materials suitable for electronic and optoelectronic applications.

We have elaborated a library based on a semifluorinated tapered dendron[19,20] that was functionalized at its apex with a diversity of electroactive donor (D) and acceptor (A) groups, **(3,4,5)12F8G1-D/A**, (Figs 1 and 2). The resulting functional dendrons self-assemble into columns containing the optoelectronic element in their cores. For synthesis and structural analysis see the Supplementary Information. The supramolecular columns self-organize into homeotropically aligned liquid crystals with hexagonal columnar (Φ_h), centred and simple rectangular columnar ($\Phi_{r\text{-}c}$ and $\Phi_{r\text{-}s}$) morphologies (Fig. 2). We name this desirable homeotropic self-organization between electrodes 'self-processing'.

Carbazole (**D1**), naphthalene (**D2**) and pyrene (**D3** and **D4**) derivatives have been introduced at the apex as D groups and 4,5,7-trinitrofluorenone-2-carboxylic acid (TNF) as an A group (**A1**) (Fig. 1). We use a diethylene glycol or tetraethylene glycol spacer between the dendron and the D or A groups to decouple their motion and facilitate fast self-assembly. The approach is simple and allows for diverse synthetic methods, and ensures that the self-assembled D and A groups are protected from moisture by the internal compartmentalization of the column and external jacketing with a fluorinated coat (Fig. 2).

Co-assembling a D-dendron with an A-dendron incorporates an electron donor–acceptor (EDA) complex in the centre of the column (see **A1** + **D1**). Disordered amorphous polymers with A and D side groups form EDA complexes when the D-dendron (**D1**) is mixed with the A-polymer (**AP1**) and when the A-dendron (**A1**) is mixed with a D-polymer (**DP1** or **DP2**). The EDA complexes assemble into columns, which in turn self-organize into Φ_h or Φ_r liquid crystals. The repulsion between the dendron's fluorine coat and the aromatic groups is so strong that the complexed polymer is forced to reside in the centre of the column (left and right columns in Fig. 2). EDA interactions[21] rather than the previously reported covalent bonding[22] are generating a supramolecular polymer[23] with dendritic side groups. But as in the previous case[22], jacketing with dendritic side groups leads to a more ordered polymer backbone.

The self-assembly and self-organization of the material into a Φ_h (**D1**, **D2**, **D3**, **D4**, **D1** + **A1**, **A1** + **DP1**, **A1** + **DP2**), $\Phi_{r\text{-}s}$ (**D1** + **AP1**) and $\Phi_{r\text{-}c}$ (**A1**) liquid crystals was demonstrated by a combination of techniques including differential scanning calorimetry (DSC), X-ray diffraction (XRD) (Fig. 3a), thermal optical polarized microscopy (TOPM) (Fig. 3b, c) and electron diffraction (ED) (Supplementary Information). Calculations based on density and XRD measurements indicate that between 3.8 and 4.6 dendrons self-assemble into a 4.8 Å stratum of the column (Supplementary Information). These self-processed systems have a column density of 4.5×10^{12} to 5.8×10^{12} columns per square centimetre (Supplementary Information), which exceeds the active element density achieved in other systems[10] by two orders of magnitude.

Figure 1 summarizes the structures of the supramolecular assemblies and their electron mobilities (μ_e) and hole mobilities (μ_h). The field- and temperature-independent μ_e and μ_h values were determined by the time-of-flight (TOF) method (Supplementary Information). Tapered D-dendrons lead to μ_h ranging from 10^{-4} to 10^{-3} $cm^2 V^{-1} s^{-1}$ in the liquid crystal state whereas the A-dendron (**A1**) has an μ_e of 10^{-3} $cm^2 V^{-1} s^{-1}$. The mobilities μ of the EDA polymer complexes are in the same range. All these values are two to five orders of magnitude higher than those of the related D and A compounds in the amorphous state (Fig. 1), reflecting the π-stacked one-dimensional ordered structure of the D, A or EDA complexes in the centre of the supramolecular column. The charge migration through the columns is not well understood but may involve a polaron hopping process[16,24]. XRD and ^{1}H-nuclear magnetic resonance (NMR) studies carried out in solution and bulk by using previously developed techniques[25] demonstrate π–π-interactions between the D or A groups. The μ value of these very simple D-dendrons are similar to those of more complex discotic liquid crystals[13–16] produced from disc-like molecules; reports of discotic liquid crystals exhibiting higher μ values[13,15,26,27] refer either to measurements on the Φ_{ho} crystal phase, or to measurements of the one-dimensional intracolumnar mobility by contactless pulse-radiolysis time-resolved microwave conductivity (PR-TRMC)[13,15,26,27]. TOF data are inherently lower owing to structural imperfections within the inter-electrode gap, but are more relevant

for technical applications than the higher values obtained by PR-TRMC.

Cooling the liquid crystal state leads to crystallization in the case of **D2**, whereas the two-dimensional (2D) order of **D1**, **D3** and **A1** is enhanced in the glassy state showing helical short-range order. For example, the XRD of a fibre of **A1** in the glassy ordered state cooled from the liquid crystal phase exhibits, in the small-angle region, the pattern of the Φ_h order (Fig. 3a). This demonstrates that the liquid crystal order of the large and uniform homeotropic domain (100 μm to a few centimetres in size) obtained by slow cooling on

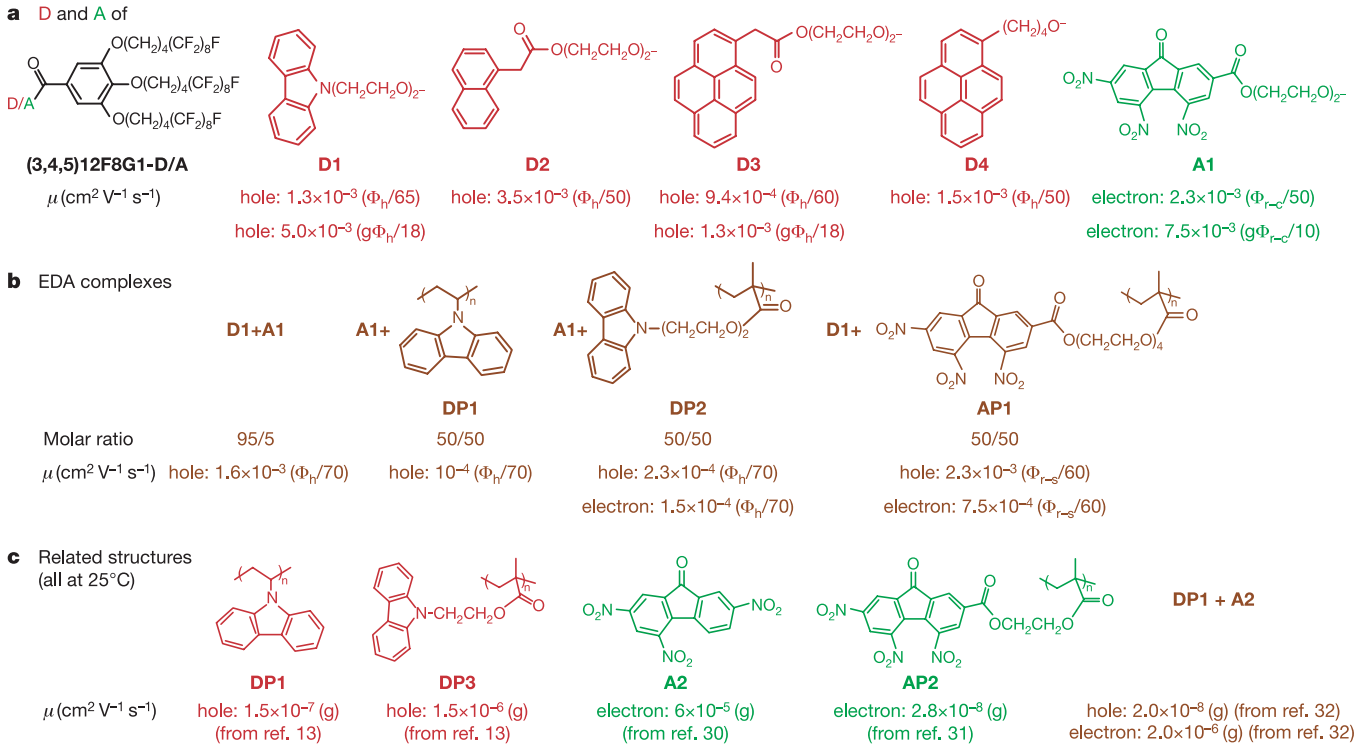

Figure 1 Charge carrier mobility of supramolecular columns and related systems. **a**, Donor (**D1–4**) and acceptor (**A1**) groups of **(3,4,5) 12F8G1-D/A**. **b**, EDA complexes. **P**, polymer. **c**, Related structures (all at 25 °C). The charge carrier mobility values (μ) are shown for all structures. (Φ_h/65), in hexagonal columnar phase at 65 °C. ($\Phi_{r\text{-}c}$/50), in centred rectangular phase at 50 °C. (gΦ_h/18), in glassy hexagonal columnar phase at 18 °C. (g$\Phi_{r\text{-}c}$/10), in glassy centred rectangular phase at 10 °C. ($\Phi_{r\text{-}s}$/60), in simple rectangular phase at 60 °C. (g), glassy.

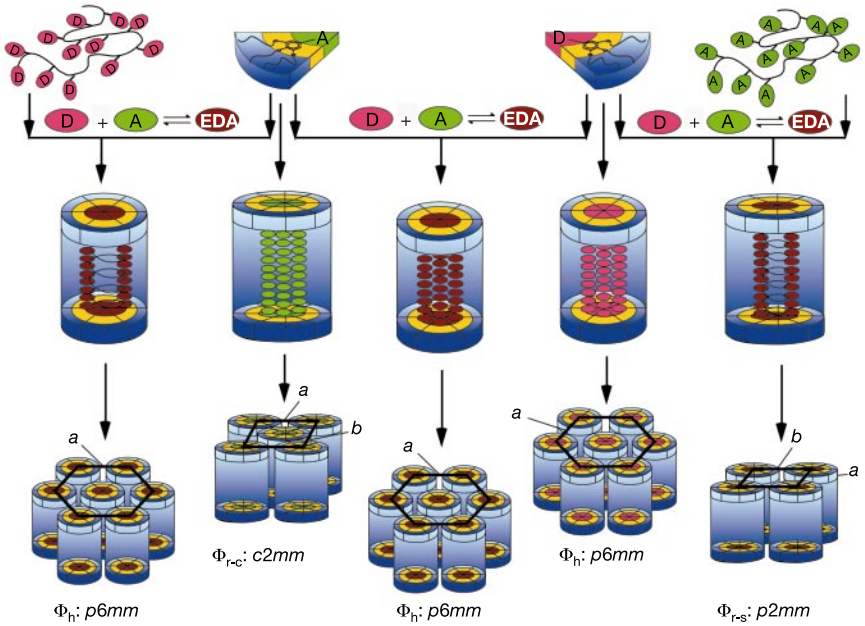

Figure 2 Schematic illustration of the liquid crystal assembly processes. Shown are the self-assembly, co-assembly and self-organization of dendrons containing donor (D) and acceptor (A) groups with each other and with disordered amorphous polymers containing D and A side groups. The different systems form hexagonal columnar (Φ_h), centred rectangular columnar ($\Phi_{r\text{-}c}$) and simple rectangular columnar ($\Phi_{r\text{-}s}$) liquid crystals. *a* and *b* are lattice dimensions; space groups are shown.

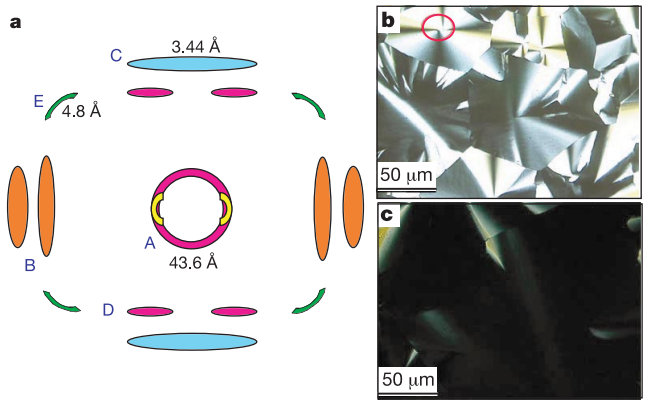

Figure 3 Structural characterization of self-assembled liquid crystals. **a**, Characteristic small- and wide-angle XRD of **A1**. The individual XRD features are identified as (A) supramolecular column to column distance, short-range, (B) order in tail region within a supramolecular cylinder, (C) π-stacks within the column, (D) correlation along a direction at an angle to the supramolecular column axis, (E) helical correlation. **b**, Thermal optical polarized micrograph (TOPM) of **D4** in the Φ_h liquid crystal state, obtained by cooling at 20 °C min^{-1} from the isotropic phase on a hydrophobic indium–tin oxide coated substrate showing defecting alignment. The circle indicates a highly tilted defect characteristic of the Φ_h phase. **c**, TOPM of a homeotropically aligned **D4**, obtained by cooling at 0.1 °C min^{-1} on the same substrate. Hydrophilic substrates such as plasma-treated carbon induce planar orientation of the columns.

a hydrophobic substrate from the isotropic state (Fig. 3b, c and Figure S3 of the Supplementary Information) is frozen into a glassy Φ_h state. In addition, at wide angles the XRD pattern reveals diffuse spots arranged in an X-like fashion that indicates short-range helical correlation along the column axis with an average repeat distance of 4.8 ± 0.3 Å (E, Fig. 3a). This value arises from the packing of the aromatic regions of the dendron near the aliphatic tails. This XRD also shows diffuse spots assigned to disordered π-stacks of TNF units in the core of the column with an average separation of 3.44 Å (C, Fig. 3a). Consequently, μ of this glassy liquid crystal state increases since the motion of the D groups from the core of the supramolecular column is decreased leading to reduced dynamic disorder (Fig. 1). Furthermore, the motion of the ionic impurities is frozen in the ordered state, whereas the photo-generated charges continue to migrate within the system. Therefore, the glassy ordered state is insensitive to ionic impurities.

Figure 4 depicts ^{1}H NMR spectra of **A1** in $CDCl_3$ solution at 22 °C, in the isotropic melt at 120 °C, in the Φ_h liquid crystal state at 75 °C and in the Φ_h glassy state at 25 °C. In this sequence, the loss of molecular mobility is reflected by the increase of the line widths. As fast magic-angle spinning is applied (except for the solution), four groups of ^{1}H resonances can be distinguished in all spectra: aromatic fluorenone (9–8 p.p.m.), dendron phenyl (7–6 p.p.m.), OCH_2 (4.5–3 p.p.m.) and alkyl (2.5–1 p.p.m.). In the glass, the liquid crystal phase and the melt, the lines are shifted to high field by about 0.5–0.7 p.p.m. relative to the solution-state values except for the alkyl resonances. This effect is due to aromatic π-electrons situated above or below the respective protons[25] and, thus, provides direct evidence for π–π packing of the fluorenones and the dendron phenyls. Analogous effects are observed in the ^{1}H spectra of the other materials discussed here. Moreover, in **A1** a distance of 3.5 Å was determined between the protons in adjacent fluorenone moieties by ^{1}H-^{1}H double-quantum NMR spectroscopy[25], which leads to the assumption of a sandwich-type packing of pairs of nitro-fluorenone groups (Fig. 5a). Combining the NMR information with the XRD data, it can be concluded that, in the glassy Φ_h phase, the columns adopt a supramolecular structure of the form

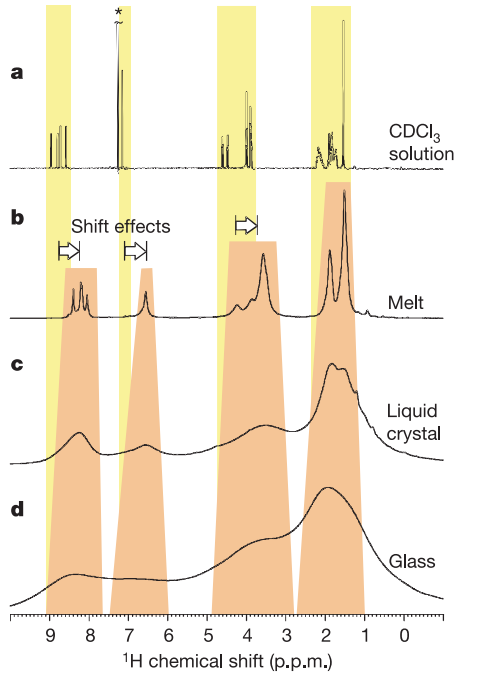

Figure 4 ^{1}H NMR spectra of **A1**. **a**, In $CDCl_3$ at 22 °C; **b**, in the isotropic melt at 120 °C; **c**, in the Φ_h liquid crystal state at 75 °C; and **d**, in the Φ_h glassy state at 25 °C. Spectra **b**–**d** were recorded under fast magic-angle spinning. The high-field shifts caused by adjacent π-electron systems are indicated by arrows.

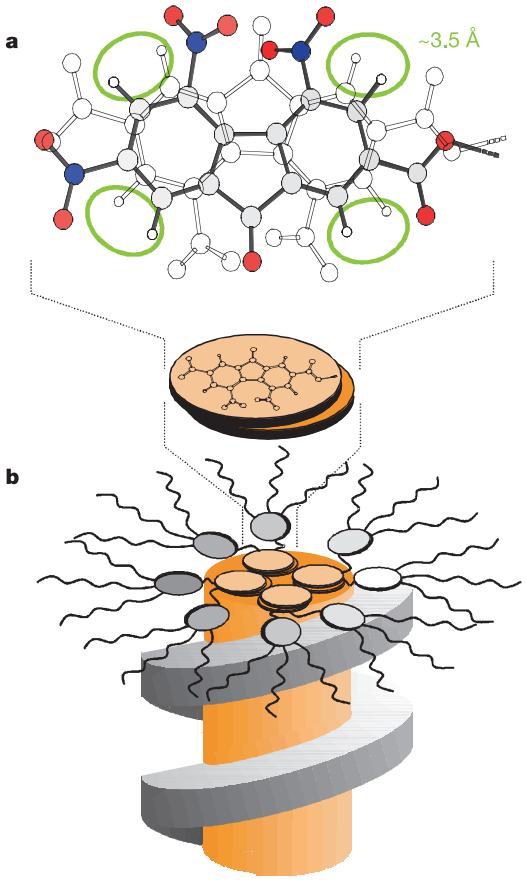

Figure 5 The molecular arrangement in the supramolecular column self-assembled from **A1**. **a**, Sandwich-type stacking of the nitro-fluorenone moieties with proton–proton distances of 3.5 Å, as determined by ^{1}H-^{1}H double-quantum NMR spectroscopy. **b**, Structure of the supramolecular columns with stacks of fluorenone sandwiches in the centre of the columns, jacketed by helical dendrons.

schematically depicted in Fig. 5b. In the centre, the fluorenone sandwiches are stacked in a column surrounded by dendrons whose phenyl groups are arranged in a helical fashion around the central column. Furthermore, NMR data indicate separation of the fluorenones (centre), dendron phenyls (inner ring) and alkyl chains (outer ring) from each other, because there are no proton–proton distances detectable between the different units on a length scale of <4 Å. This clear separation is not completely achieved when the material is precipitated from solution, but only when the system is allowed to self-organize during slow cooling from the melt into the liquid crystal and glassy Φ_h phases. Before this cooling and 'self-repair' process, the supramolecular column contains defects introduced by intramolecular backfolded **A1** dendrons.

The supramolecular arrangement shown in Fig. 5b resembles the base-pairing in DNA, which is known to support charge migration[28], and points to a new structural framework for incorporating dendritic molecules into functional materials[29]. □

Received 5 June; accepted 16 August 2002; doi:10.1038/nature01072.

1. Pope, M. & Swenberg, C. E. *Electronic Processes in Organic Crystals and Polymers* (Oxford Univ. Press, Oxford, 1999).
2. Shirakawa, H. The discovery of polyacetylene film: the dawning of an era of conducting polymers. *Angew. Chem. Int. Edn* **40,** 2574–2580 (2001).
3. MacDiarmid, A. G. Synthetic metals: a novel role for organic polymers. *Angew. Chem. Int. Edn* **40,** 2581–2590 (2001).
4. Heeger, A. J. Semiconducting and metallic polymers: the fourth generation of polymeric materials. *Angew. Chem. Int. Edn* **40,** 2591–2611 (2001).
5. Sirringhaus, H., Tessler, N. & Friend, R. H. Integrated optoelectronic devices based on conjugated polymers. *Science* **280,** 1741–1744 (1998).
6. Sirringhaus, H. *et al.* Two-dimensional charge transport in self-organized, high-mobility conjugated polymers. *Nature* **401,** 685–688 (1999).
7. Katz, H. E., Bao, Z. & Gilat, S. L. Synthetic chemistry for ultrapure, processable and high-mobility organic transistor semiconductors. *Acc. Chem. Res.* **34,** 359–369 (2001).
8. Würthner, F. Plastic transistors reach maturity for mass applications in microelectronics. *Angew. Chem. Int. Edn* **40,** 1037–1039 (2001).
9. Katz, H. E. *et al.* A soluble and air-stable organic semiconductor with high electron mobility. *Nature* **404,** 478–481 (2000).
10. Thurn-Albrecht, T. *et al.* Ultrahigh-density nanowire arrays in self-assembled diblock copolymer templates. *Science* **290,** 2126–2129 (2000).
11. Meyer zu Heringdorf, F.-J., Reuter, M. C. & Tromp, R. M. Growth dynamics of pentacene thin films. *Nature* **412,** 517–520 (2000).
12. Uryu, T., Ohkawa, H. & Oshima, R. Synthesis and high hole mobility of isotactic poly(2-N-carbazolylethyl acrylate). *Macromolecules* **20,** 712–716 (1987).
13. Adam, D. *et al.* Fast photoconduction in the highly ordered columnar phase of a discotic liquid crystal. *Nature* **371,** 141–143 (1994).
14. Kreouzis, T. *et al.* Enhanced electronic transport properties in complementary binary discotic liquid crystal systems. *Chem. Phys.* **262,** 489–497 (2000).
15. van de Craats, A. M. & Warman, J. M. The core-size effect on the mobility of charge in discotic liquid crystalline materials. *Adv. Mater.* **13,** 130–133 (2001).
16. Kreouzis, T. *et al.* Temperature-independent hole mobility in discotic liquid crystals. *J. Chem. Phys.* **114,** 1797–1802 (2001).
17. Schmidt-Mende, L. *et al.* Self-organized discotic liquid crystals for high-efficiency organic photovoltaics. *Science* **293,** 1119–1122 (2001).
18. Funahashi, M. & Hanna, J. Fast hole transport in a new calamitic liquid crystal of 2-(4′-heptyloxyphenyl)-6-dodecylthiobenzothiazole. *Phys. Rev. Lett.* **78,** 2184–2187 (1997).
19. Percec, V., Johansson, G., Ungar, G. & Zhou, J. Fluorophobic effect induces the self-assembly of semifluorinated tapered monodendrons containing crown ethers into supramolecular columnar dendrimers which exhibit a homeotropic hexagonal columnar liquid crystalline phase. *J. Am. Chem. Soc.* **118,** 9855–9866 (1996).
20. Hudson, S. D. *et al.* Direct visualization of individual cylindrical and spherical supramolecular dendrimers. *Science* **278,** 449–452 (1997).
21. Rodriguez-Parada, J. M. & Percec, V. Interchain electron-donor complexes: a model to study polymer-polymer miscibility. *Macromolecules* **19,** 55–64 (1986).
22. Percec, V. *et al.* Controlling polymer shape through the self-assembly of dendritic side-groups. *Nature* **391,** 161–164 (1998).
23. Lehn, J.-M. Toward complex matter: supramolecular chemistry and self-organization. *Proc. Natl Acad. Sci. USA* **99,** 4763–4768 (2002).
24. Shiyanovskaya, I., Singer, K. D., Twieg, R. J., Sukhomlinova, L. & Gettwert, V. Electronic transport in smectic liquid crystals. *Phys. Rev. E.* **65,** 041715 (2002).
25. Brown, S. P., Schnell, I., Brand, J. D., Müllen, K. & Spiess, H. W. An investigation of π-π packing in a columnar hexabenzocoronene by fast magic-angle spinning and double-quantum ^{1}H solid-state NMR spectroscopy. *J. Am. Chem. Soc.* **121,** 6712–6718 (1999).
26. van de Craats, A. M., de Haas, M. P. & Waarman, J. M. Charge carrier mobilities in the crystalline solid and discotic mesophases of hexakis-hexylthio and hexakis-hexyloxy triphenylene. *Synth. Met.* **86,** 2125–2126 (1997).
27. Fontes, E., Heiney, P. A. & de Jeu, W. H. Liquid-crystalline and helical order in a discotic mesophase. *Phys. Rev. Lett.* **61,** 1202–1205 (1988).
28. Ratner, M. Electronic motion in DNA. *Nature* **397,** 480–481 (1999).
29. Tomalia, D. A. & Fréchet, J. M. J. Discovery of dendrimers and dendritic polymers: A brief personal perspective. *J. Polym. Sci. A Polym. Chem.* **40,** 2719–2728 (2002).
30. Emerald, R. L. & Mort, J. Transient photoinjection of electrons from amorphous selenium into trinitrofluorenone. *J. Appl. Phys.* **45,** 3943–3945 (1974).
31. Turner, S. R. Synthesis, charge transfer complex behavior, and electronic transport properties of novel electron-acceptor polymers based on trinitrofluorenone. *Macromolecules* **13,** 782–785 (1980).
32. Gill, W. D. Drift mobilities in amorphous charge-transfer complexes of trinitrofluorenone and poly-n-vinylcarbazole. *J. Appl. Phys.* **43,** 5033–5040 (1972).

Supplementary Information accompanies the paper on *Nature*'s website (http://www.nature.com/nature).

Acknowledgements

We thank S. Z. D. Cheng for density measurements. Financial support by the National Science Foundation, the Air Force Office of Scientific Research, the Army Research Office-Multidisciplinary University Research Initiatives and the Office of Naval Research (all USA), Bundesministerium für Bildung und Forschung (Germany), and a Humboldt research award (to V.P.) is gratefully acknowledged.

Competing interests statement

The authors declare that they have no competing financial interests.

Correspondence and requests for materials should be addressed to V.P. (e-mail: percec@sas.upenn.edu).

Copepod hatching success in marine ecosystems with high diatom concentrations

Xabier Irigoien*, Roger P. Harris†, Hans M. Verheye‡, Pierre Joly§, Jeffrey Runge§‖, Michel Starr§, David Pond¶, Robert Campbell#, Rachael Shreeve¶, Peter Ward¶, Amy N. Smith☆, Hans G. Dam☆, William Peterson, Valentina Tirelli††, Marja Koski‡‡, Tania Smith†, Derek Harbour† & Russell Davidson§§**

* *AZTI- Arrantza eta Elikaigintzarako Institutu Teknologikoa, Herrera Kaia portualdea z/g 20110 Pasaia, Spain*
† *Plymouth Marine Laboratory, Prospect Place, Plymouth PL1 3DH, UK*
‡ *Marine & Coastal Management, Private Bag X2, Rogge Bay 8012, Cape Town, South Africa*
§ *Institut Maurice Lamontagne, 850 Route de la Mer, Mont Joli, Quebec, G5H 3Z4, Canada*
¶ *British Antarctic Survey, Madingley Road, Cambridge CB3 0ET, UK*
# *School of Earth and Ocean Sciences, University of Victoria, PO 3055 Stn CSC, Victoria, British Columbia, V8W 3P6, Canada*
☆ *Department of Marine Sciences, University of Connecticut, 1080 Shennecosset Rd, Groton, Connecticut 06340, USA*
** *National Marine Fisheries Service, 2030 S. Marine Science Drive, Newport, Oregon 97365, USA*
†† *Department of Biology-University of Trieste and LBM, Via Weiss 2, Trieste, Italy*
‡‡ *Netherlands Institute of Sea Research, PO Box 59, Den Burg 1790 AB, The Netherlands*
§§ *Southampton Oceanography Centre, European Way, Southampton SO14 3ZH, UK*

Diatoms dominate spring bloom phytoplankton assemblages in temperate waters and coastal upwelling regions of the global ocean. Copepods usually dominate the zooplankton in these regions and are the prey of many larval fish species. Recent laboratory studies suggest that diatoms may have a deleterious effect on the success of copepod egg hatching[1–4]. These findings challenge the classical view of marine food-web energy flow from diatoms to fish by means of copepods[5–7]. Egg mortality is an important factor in copepod population dynamics[8], thus, if diatoms have a deleterious *in situ* effect, paradoxically, high

‖ Present address: Ocean Process Analysis Laboratory, 142 Morse Hall, University of New Hampshire, Durham, New Hampshire 03824, USA.